

Scotoseesaw model implied by dark right-handed neutrinos

Phung Van Dong* and Duong Van Loi†

Phenikaa Institute for Advanced Study and Faculty of Basic Science,

Phenikaa University, Yen Nghia, Ha Dong, Hanoi 100000, Vietnam

(Dated: November 17, 2023)

We find a dark gauge symmetry $U(1)_D$ that transforms nontrivially only for three right-handed neutrinos $\nu_{1,2,3R}$. The anomaly cancellation demands that they have a dark charge $D = 0, -1, +1$ assigned to $\nu_{1,2,3R}$, respectively. The dark charge is broken by two units down to a dark parity, i.e. $U(1)_D \rightarrow P_D = (-1)^D$, which stabilizes a dark matter candidate. Interestingly, the model manifestly supplies neutrino masses via joint seesaw and scotogenic mechanisms, called scotoseesaw.

I. MOTIVATION

The standard model arranges left-handed fermions in doublets, $l_{aL} \equiv (\nu_{aL}, e_{aL})$ and $q_{aL} \equiv (u_{aL}, d_{aL})$, while it puts right-handed fermion partners in singlets, e_{aR} , u_{aR} , and d_{aR} , where $a = 1, 2, 3$ is a family index. Since the standard model contains neither sterile right-handed neutrino singlets nor lepton number violating interactions, it implies massless neutrinos in contrast with experiment [1, 2].

If right-handed neutrinos ν_{aR} are included according to respective families, possessing large Majorana masses M 's that couple ν_R 's by themselves, it leads to canonical seesaw mechanism producing appropriate neutrino masses, suppressed by $m_\nu \simeq -m^2/M$ where Dirac neutrino masses m 's linking ν_L with ν_R are proportional to the weak scale, obeying $m \ll M$ [3–7]. However, the canonical seesaw mechanism in itself does not manifestly explain the existence of dark matter, similarly to the standard model [8, 9].

If right-handed neutrinos ν_R 's are odd under an exact symmetry Z_2 , the Dirac masses m 's are suppressed, while the Majorana masses M 's are allowed. Additionally, the left-handed neutrinos ν_L 's only couple to ν_R 's via an inert Higgs doublet η that is odd under Z_2 too. In this way, neutrino masses are radiatively induced by dark fields ν_R 's and η^0 's that run in the

* dong.phungvan@phenikaa-uni.edu.vn (corresponding author)

† loi.duongvan@phenikaa-uni.edu.vn

loop, called scotogenic mechanism [10]. This approach is well motivated since the lightest of dark fields ν_R 's and η^0 's is stabilized by Z_2 responsible for dark matter. However, the existence of the Z_2 symmetry—which is *ad hoc* input—is a mystery.

The Z_2 symmetry arises as a residual matter parity from gauged $B-L$ (see, e.g., [11, 12]); alternatively, it results from breaking of a dark gauge charge (see, e.g., [13, 14]). To our best knowledge, most gauge extensions of the scotogenic setup that properly stabilizes a dark matter candidate require extra degrees of fermions of freedom beyond the conventional three right-handed neutrinos—the counterparts of usual neutrinos.

This work looks for a novel dark (gauge) symmetry that governs just three right-handed neutrinos as in the minimal scotogenic setup, by contrast. Interestingly, dark symmetry breaking implies neutrino mass generation and dark matter stability as interplay between canonical seesaw and scotogenic scheme, so-called scotoseesaw.

Let us remind the reader that the simplest scotoseesaw set by two right-handed neutrinos was first studied in [15] and late in [16] by *ad hoc* imposing an anomalous $U(1)$ or a Z_2 symmetry, by contrast. And, this scheme has been extensively studied in [17–20]. Hence, our proposal indicates that a gauge completion of scotoseesaw requires at least three right-handed neutrinos in order for it properly working.

II. PROPOSAL

This work for the first time assumes that the three right-handed neutrinos ν_{aR} ($a = 1, 2, 3$) by themselves transform nontrivially under a dark gauge symmetry $U(1)_D$, i.e. ν_{aR} each is assigned to a dark charge D_a according to $a = 1, 2, 3$, whereas all the standard model fields possess $D = 0$. The cancellation of $[\text{Gravity}]^2 U(1)_D$ and $[U(1)_D]^3$ anomalies constrains $D_1 + D_2 + D_3 = 0$ and $D_1^3 + D_2^3 + D_3^3 = 0$, respectively. It leads to $D_1 = 0$, $D_2 = -1$, and $D_3 = +1$ to be the unique solution, if indistinguishing $\nu_{1,2,3R}$ and normalizing the nonzero charge to unity, without loss of generality. Indeed, since $U(1)_D$ theory is invariant under a scale symmetry $D \rightarrow cD$ for charge and $g_D \rightarrow g_D/c$ for coupling, one can choose c so that the charge normalization takes place.

Further, ν_{1R} couples to leptons via usual Higgs doublet H , while $\nu_{2,3R}$ couple to leptons via new Higgs doublets η, χ with charge $D = +1, -1$, respectively. D -charge is broken by a new Higgs singlet ϕ with charge $D = 2$, which couples to $\nu_{2,3R}$ generating Majorana masses

Field	$SU(3)_C$	$SU(2)_L$	$U(1)_Y$	$U(1)_D$	P_D
$l_{aL} = \begin{pmatrix} \nu_{aL} \\ e_{aL} \end{pmatrix}$	1	2	-1/2	0	+
ν_{1R}	1	1	0	0	+
ν_{2R}	1	1	0	-1	-
ν_{3R}	1	1	0	+1	-
e_{aR}	1	1	-1	0	+
$q_{aL} = \begin{pmatrix} u_{aL} \\ d_{aL} \end{pmatrix}$	3	2	1/6	0	+
u_{aR}	3	1	2/3	0	+
d_{aR}	3	1	-1/3	0	+
$H = \begin{pmatrix} H^+ \\ H^0 \end{pmatrix}$	1	2	1/2	0	+
$\eta = \begin{pmatrix} \eta^0 \\ \eta^- \end{pmatrix}$	1	2	-1/2	+1	-
$\chi = \begin{pmatrix} \chi^0 \\ \chi^- \end{pmatrix}$	1	2	-1/2	-1	-
ϕ	1	1	0	2	+

TABLE I. Field presentation content of the model.

for $\nu_{2,3R}$ too. Notice that ν_{1R} can pick up a Majorana mass by itself, unsuppressed by any symmetry. It is noteworthy that D -charge is broken by two units due to $\langle\phi\rangle$ down to a residual dark parity $P_D = (-1)^D$. Particle representation content under the full gauge symmetry and residual dark parity is collected to Tab. I for brevity. The dark parity conservation implies that η, χ have vanishing VEVs, while H, ϕ develop VEVs, $\langle H \rangle = (0, v/\sqrt{2})$ and $\langle \phi \rangle = \Lambda/\sqrt{2}$, such that $\Lambda \gg v = 246$ GeV for consistency with the standard model.

It is further stressed that the neutrinos gain a suitable mass via a so-called scotoseesaw mechanism as described by Feynman diagrams in Fig. 1. The tree-level diagram is a part of the canonical seesaw governed by ν_{1R} , while the loop-level diagrams are a part of the scotogenic scheme set by $\nu_{2,3R}$. For comparison, the latter that contains Majorana fermions

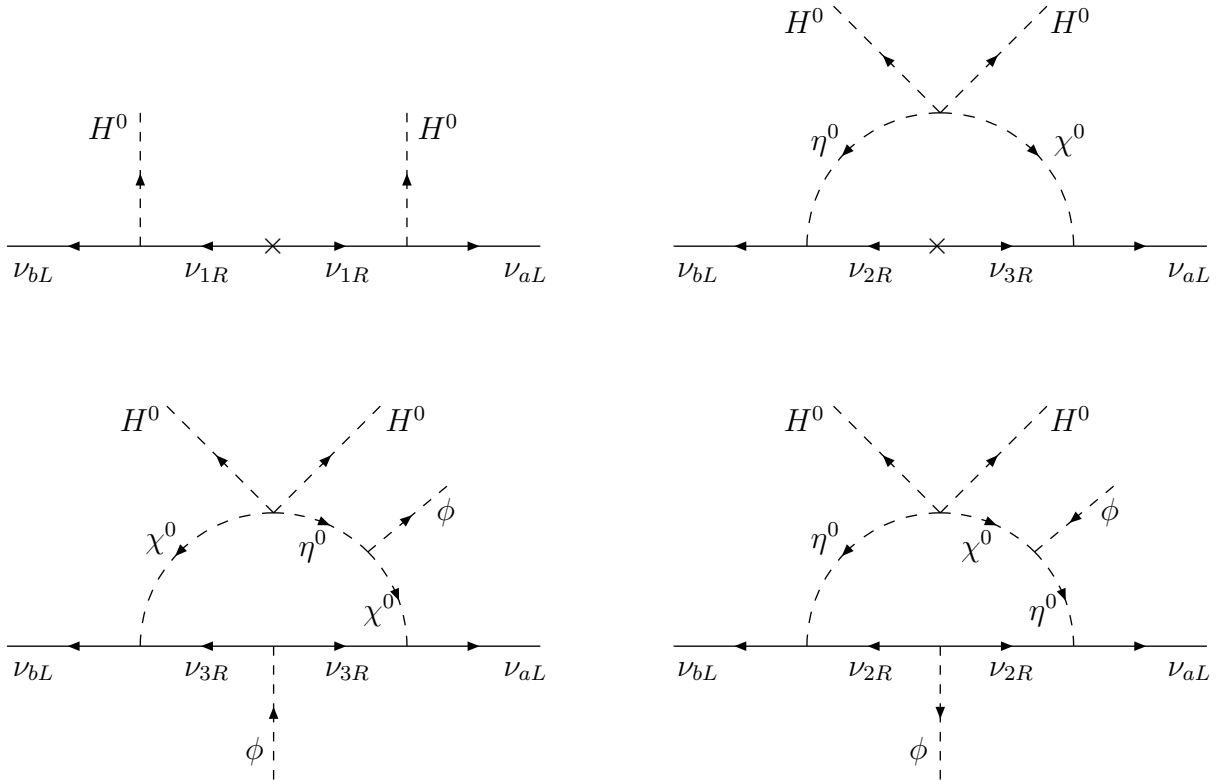


FIG. 1. Scotoseesaw neutrino mass generation governed by dark gauge symmetry, where interchanging vertices of ν_{aL} and ν_{bL} leads to three new one-loop diagrams (unplotted).

in the loop differs from [13] which interprets Dirac fermions by contrast. Additionally, the present scotoseesaw recognized for three families naturally arises as a result of dark charge breaking, significantly overhauling the simplest models previously studied in [15, 16]. Let us remind the reader that a recent approach [21] based upon gauged $B - L$ that assigns $B - L = -4, -4, +5$ to $\nu_{1,2,3R}$ also hints at existence of the scotoseesaw; furthermore, the scotogenic part may alternatively come from [22].

III. SCALAR POTENTIAL

We decomposes the scalar potential into $V = V(H, \phi) + V(\eta, \chi, \text{mix})$, where the first part includes the normal fields that induce gauge symmetry breaking,

$$V(H, \phi) = \mu_1^2 H^\dagger H + \mu_2^2 \phi^* \phi + \lambda_1 (H^\dagger H)^2 + \lambda_2 (\phi^* \phi)^2 + \lambda_3 (H^\dagger H)(\phi^* \phi), \quad (1)$$

while the second part contains the dark fields and their couplings with normal fields,

$$\begin{aligned}
V(\eta, \chi, \text{mix}) = & \mu_3^2 \eta^\dagger \eta + \mu_4^2 \chi^\dagger \chi + \lambda_4 (\eta^\dagger \eta)^2 + \lambda_5 (\chi^\dagger \chi)^2 + \lambda_6 (\eta^\dagger \eta) (\chi^\dagger \chi) + \lambda_7 (\eta^\dagger \chi) (\chi^\dagger \eta) \\
& + (\lambda_8 \eta^\dagger \eta + \lambda_9 \chi^\dagger \chi) (H^\dagger H) + \lambda_{10} (\eta^\dagger H) (H^\dagger \eta) + \lambda_{11} (\chi^\dagger H) (H^\dagger \chi) \\
& + (\lambda_{12} \eta^\dagger \eta + \lambda_{13} \chi^\dagger \chi) (\phi^* \phi) + [\lambda_{14} (H \eta) (H \chi) + \mu_5 (\eta^\dagger \chi) \phi + H.c.]. \quad (2)
\end{aligned}$$

Hereafter, λ_{14} and μ_5 are assumed to be real, since otherwise their phases can be absorbed by redefining appropriate scalar fields. The expected vacuum structure acquires $\mu_{1,2}^2 < 0$ and $\mu_{3,4}^2 > 0$. Additionally, necessary condition for the potential bounded from below is $\lambda_{1,2,4,5} > 0$, which is obtained by requiring $V > 0$ for H, ϕ, η, χ separately tending to infinity, respectively. Supplemental conditions would exist by requiring $V > 0$ for a number of scalar fields simultaneously tending to infinity, which is skipped for brevity.

Expanding $H^0 = (v + S + iA)/\sqrt{2}$, $\phi = (\Lambda + S' + iA')/\sqrt{2}$, $\eta^0 = (R + iI)/\sqrt{2}$, and $\chi^0 = (R' + iI')/\sqrt{2}$, we find the condition of potential minimum,

$$v^2 = \frac{2(\lambda_3 \mu_2^2 - 2\lambda_2 \mu_1^2)}{4\lambda_1 \lambda_2 - \lambda_3^2}, \quad \Lambda^2 = \frac{2(\lambda_3 \mu_1^2 - 2\lambda_1 \mu_2^2)}{4\lambda_1 \lambda_2 - \lambda_3^2}. \quad (3)$$

Physical scalar fields relevant to the normal sector are identified as

$$H = \begin{pmatrix} G_W^+ \\ \frac{1}{\sqrt{2}}(v + c_\varphi H_1 + s_\varphi H_2 + iG_Z) \end{pmatrix}, \quad \phi = \frac{1}{\sqrt{2}}(\Lambda - s_\varphi H_1 + c_\varphi H_2 + iG_{Z^0}), \quad (4)$$

where $G_W^+ \equiv H^+$, $G_Z \equiv A$, and $G_{Z^0} \equiv A'$ are massless Goldstone bosons coupled to gauge bosons W^+ , Z , and Z' , respectively. The standard model like Higgs boson $H_1 \equiv c_\varphi S - s_\varphi S'$ and the new Higgs boson $H_2 \equiv s_\varphi S + c_\varphi S'$ are determined via a S - S' mixing angle,

$$t_{2\varphi} = \frac{\lambda_3 v \Lambda}{\lambda_2 \Lambda^2 - \lambda_1 v^2} \simeq \frac{\lambda_3 v}{\lambda_2 \Lambda} \ll 1, \quad (5)$$

as well as obtaining respective masses,

$$m_{H_1}^2 = \lambda_1 v^2 + \lambda_2 \Lambda^2 - \sqrt{(\lambda_1 v^2 - \lambda_2 \Lambda^2)^2 + \lambda_3^2 v^2 \Lambda^2} \simeq \left(2\lambda_1 - \frac{\lambda_3^2}{2\lambda_2}\right) v^2, \quad (6)$$

$$m_{H_2}^2 = \lambda_1 v^2 + \lambda_2 \Lambda^2 + \sqrt{(\lambda_1 v^2 - \lambda_2 \Lambda^2)^2 + \lambda_3^2 v^2 \Lambda^2} \simeq 2\lambda_2 \Lambda^2. \quad (7)$$

Relevant to the dark scalar sector, we conveniently define $M_\eta^2 \equiv \mu_3^2 + \frac{\lambda_8}{2} v^2 + \frac{\lambda_{12}}{2} \Lambda^2$ and $M_\chi^2 \equiv \mu_4^2 + \frac{\lambda_9}{2} v^2 + \frac{\lambda_{13}}{2} \Lambda^2$. The charged dark scalars η^- and χ^- are physical fields by themselves with respective masses, obtained by

$$m_\eta^2 = M_\eta^2 + \frac{\lambda_{10}}{2} v^2, \quad m_\chi^2 = M_\chi^2 + \frac{\lambda_{11}}{2} v^2. \quad (8)$$

By contrast, the neutral dark scalars R, R' and I, I' mix in each pair, such as

$$V \supset \frac{1}{2} \begin{pmatrix} R & R' \end{pmatrix} \begin{pmatrix} M_\eta^2 & \frac{\mu_5 \Lambda}{\sqrt{2}} + \frac{\lambda_{14} v^2}{2} \\ \frac{\mu_5 \Lambda}{\sqrt{2}} + \frac{\lambda_{14} v^2}{2} & M_\chi^2 \end{pmatrix} \begin{pmatrix} R \\ R' \end{pmatrix} \\ + \frac{1}{2} \begin{pmatrix} I & I' \end{pmatrix} \begin{pmatrix} M_\eta^2 & \frac{\mu_5 \Lambda}{\sqrt{2}} - \frac{\lambda_{14} v^2}{2} \\ \frac{\mu_5 \Lambda}{\sqrt{2}} - \frac{\lambda_{14} v^2}{2} & M_\chi^2 \end{pmatrix} \begin{pmatrix} I \\ I' \end{pmatrix}. \quad (9)$$

Defining the mixing angles of the dark real and imaginary sectors,

$$t_{2\theta_R} = \frac{\sqrt{2}\mu_5\Lambda + \lambda_{14}v^2}{M_\chi^2 - M_\eta^2}, \quad t_{2\theta_I} = \frac{\sqrt{2}\mu_5\Lambda - \lambda_{14}v^2}{M_\chi^2 - M_\eta^2}, \quad (10)$$

we obtain physical fields,

$$R_1 = c_{\theta_R} R - s_{\theta_R} R', \quad R_2 = s_{\theta_R} R + c_{\theta_R} R', \quad (11)$$

$$I_1 = c_{\theta_I} I - s_{\theta_I} I', \quad I_2 = s_{\theta_I} I + c_{\theta_I} I', \quad (12)$$

with respective masses,

$$m_{R_1}^2 \simeq M_\eta^2 + \frac{\frac{1}{4}(\sqrt{2}\mu_5\Lambda + \lambda_{14}v^2)^2}{M_\eta^2 - M_\chi^2}, \quad m_{R_2}^2 \simeq M_\chi^2 - \frac{\frac{1}{4}(\sqrt{2}\mu_5\Lambda + \lambda_{14}v^2)^2}{M_\eta^2 - M_\chi^2}, \quad (13)$$

$$m_{I_1}^2 \simeq M_\eta^2 + \frac{\frac{1}{4}(\sqrt{2}\mu_5\Lambda - \lambda_{14}v^2)^2}{M_\eta^2 - M_\chi^2}, \quad m_{I_2}^2 \simeq M_\chi^2 - \frac{\frac{1}{4}(\sqrt{2}\mu_5\Lambda - \lambda_{14}v^2)^2}{M_\eta^2 - M_\chi^2}, \quad (14)$$

where the approximations assume $\mu_5\Lambda \sim \lambda_{14}v^2 \ll M_{\eta,\chi}^2 \sim \Lambda^2$, thus $\mu_5 \ll \Lambda$. It is clear that R_1, I_1 , as well as R_2, I_2 , are now separated in mass, namely $(m_{R_i}^2 - m_{I_i}^2)/(m_{R_i}^2 + m_{I_i}^2) \sim \lambda_{14}^2(v/\Lambda)^4 \ll 1$, for $i = 1, 2$. It is stressed that this mass splitting is in the same magnitude with the mixing angles-squared, $\theta_{R,I}^2 \sim \lambda_{14}^2(v/\Lambda)^4 \ll 1$.

IV. NEUTRINO MASS

Every charged lepton and quark gain an appropriate mass through interacting with the Higgs field H identical to the standard model. Concerning left-handed and right-handed neutrinos, their Yukawa Lagrangian is given by

$$\mathcal{L} \supset h_{a1}\bar{l}_{aL}\tilde{H}\nu_{1R} + h_{a2}\bar{l}_{aL}\eta\nu_{2R} + h_{a3}\bar{l}_{aL}\chi\nu_{3R} \\ - \frac{1}{2}M_1\bar{\nu}_{1R}^c\nu_{1R} + \frac{1}{2}f_2\bar{\nu}_{2R}^c\nu_{2R}\phi + \frac{1}{2}f_3\bar{\nu}_{3R}^c\nu_{3R}\phi^* - M_{23}\bar{\nu}_{2R}^c\nu_{3R} + H.c. \quad (15)$$

When H, ϕ develop VEVs, we obtain a tree-level mass Lagrangian,

$$\mathcal{L} \supset -\frac{1}{2} \begin{pmatrix} \bar{\nu}_{aL} & \bar{\nu}_{1R}^c \end{pmatrix} \begin{pmatrix} 0 & m_{a1} \\ m_{b1} & M_1 \end{pmatrix} \begin{pmatrix} \nu_{bL}^c \\ \nu_{1R} \end{pmatrix} - \frac{1}{2} \begin{pmatrix} \bar{\nu}_{2R}^c & \bar{\nu}_{3R}^c \end{pmatrix} \begin{pmatrix} M_2 & M_{23} \\ M_{23} & M_3 \end{pmatrix} \begin{pmatrix} \nu_{2R} \\ \nu_{3R} \end{pmatrix} + H.c., \quad (16)$$

where $b = 1, 2, 3$ is a family index as a is. Additionally, $m_{a1} = -h_{a1}v/\sqrt{2}$ is a Dirac mass, while $M_2 = -f_2\Lambda/\sqrt{2}$ and $M_3 = -f_3\Lambda/\sqrt{2}$ are Majorana masses as M_1 and M_{23} are.

Without loss of generality, we assume $M_{23} = 0$, i.e. neither mixing between ν_{2R} and ν_{3R} nor the corresponding loop diagram (right-upper) in Fig. 1 exist. Diagonalizing the mass matrix of (ν_L, ν_{1R}) in (16), which has a seesaw form due to $v \ll M_1$, we get

$$\mathcal{L} \supset -\frac{1}{2} (m_\nu)_{ab}^{\text{tree}} \bar{\nu}_{aL} \nu_{bL}^c - \frac{1}{2} M_1 \bar{\nu}_{1R}^c \nu_{1R} - \frac{1}{2} M_2 \bar{\nu}_{2R}^c \nu_{2R} - \frac{1}{2} M_3 \bar{\nu}_{3R}^c \nu_{3R} + H.c., \quad (17)$$

where the first term,

$$(m_\nu)_{ab}^{\text{tree}} \simeq -\frac{m_{a1}m_{b1}}{M_1}, \quad (18)$$

is the seesaw-induced neutrino mass identically to the contribution of the tree-level diagram (left-upper) in Fig. 1, while $\nu_{1,2,3R}$ are apparently decoupled, behaving as physical Majorana fields with masses $M_{1,2,3}$, respectively.

The tree-level mass matrix (18) gives only a nonzero (mass) eigenvalue according to mass eigenstate $\sim m_{a1}\nu_{aL}$ inappropriate to experiment [23]. Interestingly, the tree-level vanished masses, or exactly the mass matrix of (ν_L, ν_{1R}) in (16), receive radiative corrections by dark fields $(\eta, \chi, \nu_{2,3R})$ as in the loop diagrams (lower-left and -right) in Fig. 1. In mass basis, the loop diagrams are commonly contributed by one of $\nu_{2,3R}$ fermions and one of $R_{1,2}, I_{1,2}$ scalars, determined by the Lagrangian,

$$\begin{aligned} \mathcal{L} \supset & \frac{h_{a2}}{\sqrt{2}} \bar{\nu}_{aL} \nu_{2R} (c_R R_1 + s_R R_2 + i c_I I_1 + i s_I I_2) \\ & + \frac{h_{a3}}{\sqrt{2}} \bar{\nu}_{aL} \nu_{3R} (-s_R R_1 + c_R R_2 - i s_I I_1 + i c_I I_2) + H.c. \end{aligned} \quad (19)$$

plus kinetic and mass terms of the relevant physical fields, where we have defined $c_R \equiv c_{\theta_R}$ and $s_R \equiv s_{\theta_R}$ for short. Therefore, the loop-induced neutrino masses are computed as

$$\begin{aligned} (m_\nu)_{ab}^{\text{rad}} = & \frac{h_{a2}h_{b2}M_2}{32\pi^2} \left(\frac{c_R^2 m_{R_1}^2 \ln \frac{M_2^2}{m_{R_1}^2}}{M_2^2 - m_{R_1}^2} - \frac{c_I^2 m_{I_1}^2 \ln \frac{M_2^2}{m_{I_1}^2}}{M_2^2 - m_{I_1}^2} + \frac{s_R^2 m_{R_2}^2 \ln \frac{M_2^2}{m_{R_2}^2}}{M_2^2 - m_{R_2}^2} - \frac{s_I^2 m_{I_2}^2 \ln \frac{M_2^2}{m_{I_2}^2}}{M_2^2 - m_{I_2}^2} \right) \\ & + \nu_{3R}\text{-contribution}, \end{aligned} \quad (20)$$

where the ν_{3R} -contribution is translated from that of ν_{2R} (previous term) by replacing $h_{a(b)2} \rightarrow h_{a(b)3}$, $M_2 \rightarrow M_3$, $c_{R,I} \rightarrow -s_{R,I}$, and $s_{R,I} \rightarrow c_{R,I}$. Notice that the divergences are manifestly cancelled out due to $c_R^2 - c_I^2 + s_R^2 - s_I^2 = 0$ for each $\nu_{2,3R}$ contribution. If the mixing between ν_{2R} and ν_{3R} is included, the above result is easily generalized by changing $h_{a(b)k} \rightarrow h_{a(b)k} U_{kl}$ for $k, l = 2, 3$, where U relates $\nu_{2,3R}$ to mass eigenstates with mass eigenvalues $M_{2,3}$ as retained, without confusion.

With the aid of dark scalar mass splittings and mixing angles, i.e. $(m_{R_i}^2 - m_{I_i}^2)/(m_{R_i}^2 + m_{I_i}^2) \sim \theta_{R,I}^2 \sim \lambda_{14}^2 (v/\Lambda)^4$ for $i = 1, 2$, we estimate the magnitude of radiative masses, $(m_\nu)^{\text{rad}} \sim 0.1 (M_{2,3}/\text{TeV}) (h\lambda_{14}/10^{-3})^2$ eV, assuming $v/\Lambda \sim 10^{-1}$, where $h \sim h_{a(b)k}$. Comparing with measured value $m_\nu \sim 0.1$ eV implies $M_{2,3} \sim \text{TeV}$ and $h\lambda_{14} \sim 10^{-3}$, thus h, λ_{14} are not too small. The last conclusion is due to a suppression in dark scalar mass splittings and mixing angles as $(v/\Lambda)^4$, which is more stronger than that of the conventional scotogenic model [10]. On the other hand, the tree-level neutrino mass in (18) obeys $(m_\nu)^{\text{tree}} \sim 0.1$ eV, indicating that either M_1 is close to the GUT scale for $h_{a1} \sim h \sim 0.1$, or alternatively h_{a1} is close to the Yukawa coupling of electron for $M_1 \sim M_{2,3} \sim \text{TeV}$. The first case is possible since M_1 is not suppressed by dark symmetry, while the second case is available too but it requires a hierarchy $h_{a1} \ll h_{ak}$ like those of the Yukawa couplings of charged leptons. In summary, the scotoseesaw neutrino mass described in Fig. 1 is given by

$$(m_\nu)_{ab} = (m_\nu)_{ab}^{\text{tree}} + (m_\nu)_{ab}^{\text{rad}}. \quad (21)$$

V. DARK MATTER

The model contains two kinds of dark matter, dark Majorana fermion ($\nu_{2,3R}$) and dark doublet scalar ($R_{1,2}, I_{1,2}$), communicated with normal matter via $U(1)_D$ gauge boson Z' and usual/new Higgs portals $H_{1,2}$. Kinetic mixing effect [24] between $U(1)_D$ and $U(1)_Y$ is too small and is not signified in this work. The dark matter candidate—the lightest of dark fields by appropriate parameter choice—is studied in order.

A. Majorana dark matter

Assuming ν_{3R} to be the lightest of dark fields, it is absolutely stabilized by the residual dark parity P_D responsible for dark matter. In the early universe, ν_{3R} 's potentially annihilate

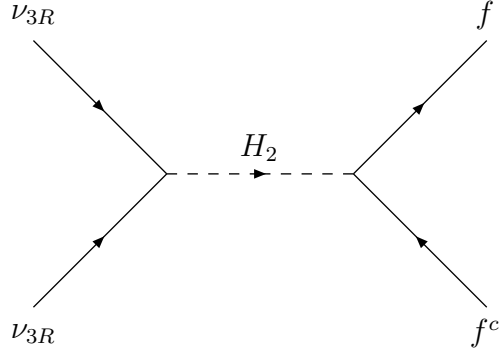


FIG. 2. Annihilation of Majorana dark matter to normal matter that sets the relic abundance.

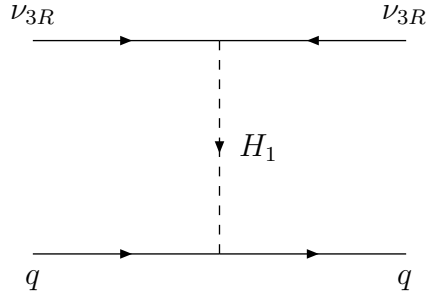


FIG. 3. Scattering of Majorana dark matter with nuclei in direct detection.

to pair of Z' —given that Z' is lighter than ν_{3R} —via t, u -channel diagrams as well as to usual fermions (ff^c) via s -channel $H_{1,2}$ portals due to a mixing between the standard model Higgs field (H) and new Higgs field (ϕ). The usual Higgs H_1 portal negligibly contributes to the relic density since ν_{3R} is heavy at TeV, necessarily set by H_2 resonance. Also, the annihilation to Z' by t, u -channels is suppressed similarly to the H_1 portal, not significantly compared to H_2 portal (cf. [25]). That said, the ν_{3R} annihilation that sets the relic density is governed by H_2 as described by the Feynman diagram in Fig. 2. Although the H_1 portal does not contribute to the relic density, it would set the spin-independent (SI) cross-section presenting scattering of ν_{3R} with nuclei in direct detection experiment as determined by the Feynman diagram in Fig. 3. This is because the H_2 contribution to the effective interaction $(\bar{\nu}_{3R}^c \nu_{3R})(\bar{q}q)$ is suppressed by $m_{H_1}^2/m_{H_2}^2 \ll 1$ as compared to that of H_1 .

The annihilation cross-section of ν_{3R} is evaluated as

$$\begin{aligned} \langle \sigma v_{\text{rel}} \rangle_{\nu_{3R}} &= \sum_f \frac{s_\varphi^2 c_\varphi^2 m_f^2 M_3^4}{8\pi v^2 \Lambda^2 (4M_3^2 - m_{H_2}^2)^2} \left(1 - \frac{m_f^2}{M_3^2} \right)^{\frac{3}{2}} \\ &\simeq \frac{s_\varphi^2 m_t^2 M_3^4}{8\pi v^2 \Lambda^2 (4M_3^2 - m_{H_2}^2)^2}, \end{aligned} \quad (22)$$

where v_{rel} is dark matter relative velocity, and the biggest contribution comes from the annihilation to top quark as enhanced by its Yukawa coupling. The usual-new Higgs mixing leads to a shift in the standard model Higgs couplings, which are well-measured at present; and, the projected HL-LHC would make stringent bounds on this shift [23]. To satisfy all the limits, we take the mixing angle to be $s_\varphi = 10^{-2}$. Additionally, let $m_t = 173$ GeV, $v = 246$ GeV, and $v/\Lambda = 0.1$. We plot the relic density $\Omega_{\nu_{3R}} h^2 \simeq 0.1 \text{ pb}/\langle \sigma v_{\text{rel}} \rangle_{\nu_{3R}}$ as function of the dark matter mass in Fig. 4 for $m_{H_2} = 2$ TeV for example. It is clear from the figure that the H_2 resonance $m_{\nu_{3R}} = \frac{1}{2}m_{H_2}$ is crucial to set the dark matter relic density.

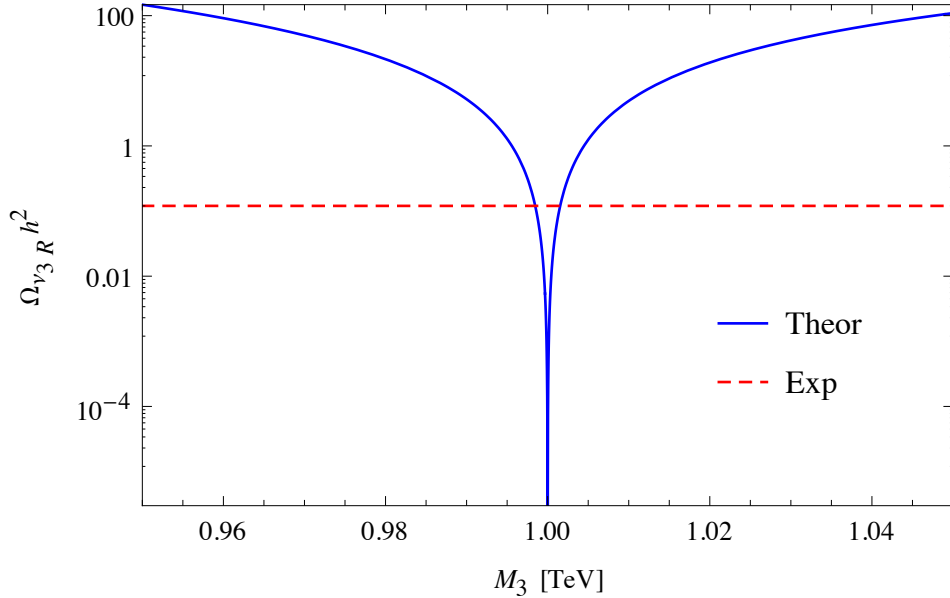


FIG. 4. Relic density of Majorana dark matter plotted as a function of its mass, where the dashed line is the measured value $\Omega_{\text{DM}} h^2 \simeq 0.12$ [23].

The effective Lagrangian describing scattering of ν_{3R} with quark is induced directly from Fig. 3 to be $\mathcal{L}_{\text{eff}} \supset \alpha_q^S (\bar{\nu}_{3R}^c \nu_{3R})(\bar{q}q)$, where

$$\alpha_q^S = -\frac{s_\varphi c_\varphi m_q M_3}{v \Lambda m_{H_1}^2}. \quad (23)$$

Hence, the scattering cross-section of dark matter with a nucleon $N = p, n$ is given by [26]

$$\sigma_{\nu_{3R}-N}^{\text{SI}} = \frac{4m_N^2}{\pi} (f^N)^2, \quad (24)$$

where the nucleon form factor obeys

$$\frac{f^N}{m_N} = \sum_{q=u,d,s} \frac{\alpha_q^S}{m_q} f_{Tq}^N + \frac{2}{27} f_{TG}^N \sum_{q=c,b,t} \frac{\alpha_q^S}{m_q} \simeq -\frac{0.35s_\varphi c_\varphi M_3}{v\Lambda m_{H_1}^2}, \quad (25)$$

where we have used $f_{TG}^N = 1 - \sum_{q=u,d,s} f_{Tq}^N$, $f_{Tu}^p = 0.02$, $f_{Td}^p = 0.026$, $f_{Ts}^p = 0.118$, $f_{Tu}^n = f_{Td}^p$, $f_{Td}^n = f_{Tu}^p$, and $f_{Ts}^n = f_{Ts}^p$ [27]. It follows that

$$\sigma_{\nu_{3R}-N}^{\text{SI}} \simeq \frac{0.49m_N^4 s_\varphi^2 M_3^2}{\pi v^2 \Lambda^2 m_{H_1}^4} \simeq \left(\frac{s_\varphi}{10^{-2}}\right)^2 \left(\frac{M_3}{\text{TeV}}\right)^2 \times 0.68 \times 10^{-46} \text{ cm}^2, \quad (26)$$

where we have taken $m_N = 1 \text{ GeV}$, $m_{H_1} = 125 \text{ GeV}$, $v = 246 \text{ GeV}$, and $v/\Lambda = 0.1$. The SI cross-section predicted is in agreement with the latest data $\sigma_{\nu_{3R}-N}^{\text{SI}} \sim 10^{-46} \text{ cm}^2$ [28] for ν_{3R} dark matter mass $M_3 \sim \text{TeV}$ and usual-new Higgs mixing $s_\varphi \sim 10^{-2}$.

B. Scalar dark matter

Since the dark scalars $R_{1,2}$ and $I_{1,2}$ are heavy at TeV, their dark matter phenomenology is quite similar to the Majorana dark matter interpreted above. Indeed, the lightest of dark fields, R_1 for instance, is now stabilized by P_D . In the early universe, it may annihilate to a pair of Z' , as well as of weak bosons, through t, u -channel diagrams or to usual fermions via $H_{1,2}$ portals. However, only the H_2 portal is enhanced due to the mass resonance that sets R_1 relic density. Concerning direct detection, R_1 scatters with nucleon via the standard model Higgs portal H_1 . The new Higgs portal gives a negligible contribution, while the Z portal is inaccessible due to the dark scalar mass splitting.

VI. CONCLUSION AND OUTLOOK

We have shown that if the three right-handed neutrinos—the right-handed partners of the usual left-handed neutrinos—possess a dark gauge charge while the standard model particles do not, their charges would be $0, -1, +1$ in order for the theory to be consistent at quantum level. This new theory implies naturally the scotoseesaw mechanism which induces appropriate neutrino masses via both contributions of DM (scotogenic) and non-DM

(seesaw) right-handed neutrinos. The dark matter candidate is either one of the dark right-handed neutrinos or one of the neutral dark scalars, obtaining a mass at TeV, possessing a correct abundance enhanced by the new Higgs mass resonance $m_{\text{DM}} = \frac{1}{2}m_{H_2}$, and potentially scattering with nucleon via the standard model Higgs exchange.

Since the present work has not signified a kinetic mixing, or this mixing is small, Z' does not significantly couple to usual fermions. Hence, the current colliders [29–31] do not make a constraint on Z' . Similarly, the other new particles, such as DM (ν_{3R} or R_1) and non-DM (ν_{1R} and H_2), would exhibit negligible signals at the present colliders because they interact rather weak with the normal matter. However, the projected HL-LHC and ILC may be worth exploring for them when the energy and sensitivity are enhanced.

-
- [1] T. Kajita, *Rev. Mod. Phys.* **88**, 030501 (2016).
 - [2] A. B. McDonald, *Rev. Mod. Phys.* **88**, 030502 (2016).
 - [3] P. Minkowski, *Phys. Lett. B* **67**, 421 (1977).
 - [4] T. Yanagida, *Conf. Proc. C* **7902131**, 95 (1979).
 - [5] M. Gell-Mann, P. Ramond, and R. Slansky, *Conf. Proc. C* **790927**, 315 (1979).
 - [6] R. N. Mohapatra and G. Senjanovic, *Phys. Rev. Lett.* **44**, 912 (1980).
 - [7] J. Schechter and J. W. F. Valle, *Phys. Rev. D* **22**, 2227 (1980).
 - [8] G. Bertone, D. Hooper, and J. Silk, *Phys. Rep.* **405**, 279 (2005).
 - [9] G. Arcadi, M. Dutra, P. Ghosh, M. Lindner, Y. Mambrini, M. Pierre, S. Profumo, and F. S. Queiroz, *Eur. Phys. J. C* **78**, 203 (2018).
 - [10] E. Ma, *Phys. Rev. D* **73**, 077301 (2006).
 - [11] E. Ma, N. Pollard, O. Popov, and M. Zakeri, *Mod. Phys. Lett. A* **31**, 1650163 (2016).
 - [12] S. K. Kang, O. Popov, R. Srivastava, J. W. F. Valle, and C. A. Vaquera-Araujo, *Phys. Lett. B* **798**, 135013 (2019).
 - [13] E. Ma, I. Picek, and B. Radovic, *Phys. Lett. B* **726**, 744 (2013).
 - [14] P. V. Dong, D. V. Loi, and D. T. Huong, *Eur. Phys. J. Plus* **138**, 753 (2023).
 - [15] J. Kubo and D. Suematsu, *Phys. Lett. B* **643**, 336 (2006).
 - [16] N. Rojas, R. Srivastava, and J. W. F. Valle, *Phys. Lett. B* **789**, 132 (2019).
 - [17] D. M. Barreiros, F. R. Joaquim, R. Srivastava, and J. W. F. Valle, *JHEP* **04**, 249 (2021).

- [18] S. Mandal, R. Srivastava, and J. W. F. Valle, *Phys. Lett. B* **819**, 136458 (2021).
- [19] J. Ganguly, J. Gluza, and B. Karmakar, *JHEP* **11**, 074 (2022).
- [20] R. Kumar, P. Mishra, M. K. Behera, R. Mohanta, and R. Srivastava, arXiv:2310.02363 [hep-ph].
- [21] J. Leite, S. Sadhukhan, and J. W. F. Valle, arXiv:2307.04840 [hep-ph].
- [22] P. V. Dong, arXiv:2305.19197 [hep-ph].
- [23] R. L. Workman *et al.* (Particle Data Group), *Prog. Theor. Exp. Phys.* **2022**, 083C01 (2022).
- [24] B. Holdom, *Phys. Lett.* **166B**, 196 (1986).
- [25] M. Fabbrichesi, E. Gabrielli, and G. Lanfranchi, arXiv:2005.01515 [hep-ph].
- [26] G. Belanger, F. Boudjema, A. Pukhov, and A. Semenov, *Comput. Phys. Commun.* **180**, 747 (2009).
- [27] J. Ellis, A. Ferstl, and K. A. Olive, *Phys. Lett. B* **481**, 304 (2000).
- [28] J. Aalbers *et al.*, *Phys. Rev. Lett.* **131**, 041002 (2023).
- [29] J. Alcaraz *et al.* (ALEPH, DELPHI, L3, OPAL Collaborations, and LEP Electroweak Working Group), arXiv:hep-ex/0612034.
- [30] G. Aad *et al.* (ATLAS Collaboration), *Phys. Lett. B* **796**, 68 (2019).
- [31] A. M. Sirunyan *et al.* (CMS Collaboration), *JHEP* **07**, 208 (2021).